

Effect of Scattering Amplitude Interference Terms On the Search for a Charged Higgs Boson

A. Arhrib, D. Azevedo, R. Benbrik, H. Harouiz,
S. Moretti, **R. Patrick**, R. Santos

The University of Adelaide

riley.patrick@adelaide.edu.au

September 13, 2019

Overview

- 1 Introduction
- 2 Benchmark Selection
- 3 Monte Carlo Modelling
- 4 Parton Level Results
- 5 Detector Level Results
- 6 Conclusion

Introduction

- Collider studies generally model Signal and Background separately.
- Define: $I = (S + B) - S - B$
- This assumption that interference is small may not hold for some areas of parameter space.

Signal to background interference in $pp \rightarrow tH^- \rightarrow tW^- b\bar{b}$ at the LHC Run-II

Abdesslam Arhrib¹, Rachid Benbrik^{2,3,4}, Stefano Moretti⁵, Rui Santos^{6,7,8} and Pankaj Sharma⁹

Figure: arxiv:1712.05018

- Interference can be of same order as signal, and sometimes negative.
- Interference large when width-mass ratio large.
- We look at $pp \rightarrow tbH^\pm \rightarrow tb\bar{t}\bar{b}$ in this study.

Current Exclusion

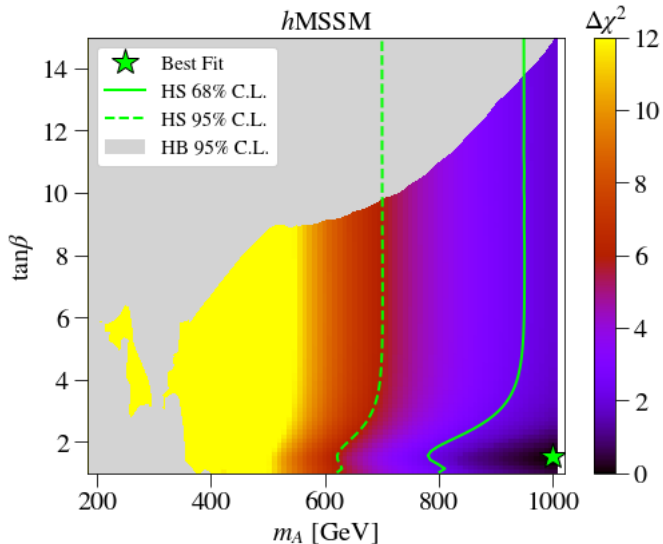


Figure: χ^2 fit sliced in the $\tan\beta$ and M_A plane in hMSSM benchmark.

Parameter Space

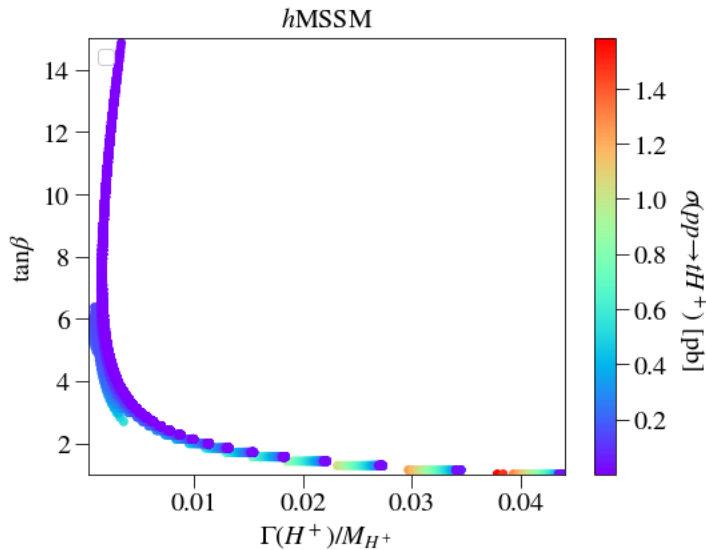


Figure: Cross section as a function of $\tan\beta$ and H^\pm width-mass ratio in hMSSM

Parameter Space

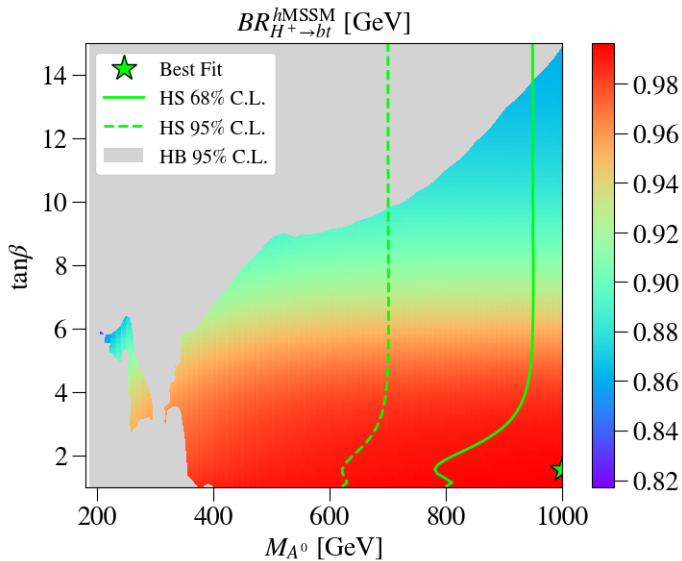


Figure: $\text{Br}(H^\pm \rightarrow tb)$ as a function of $\tan\beta$ and M_{A^0} in hMSSM benchmark.

Parameter Space

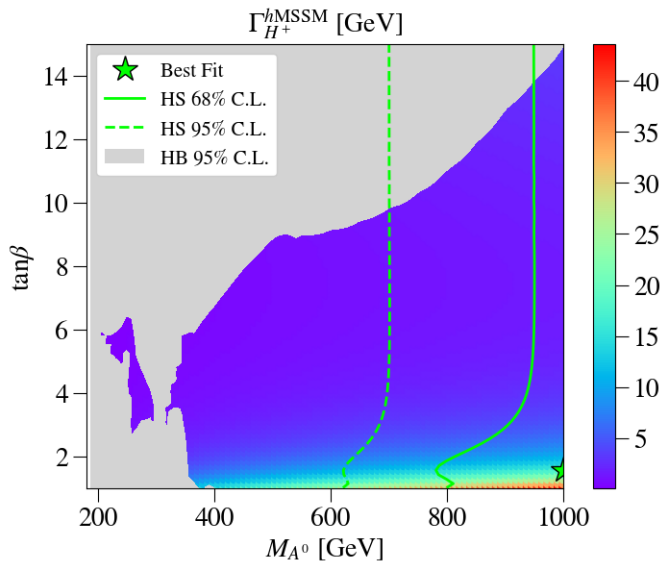


Figure: H^\pm width as a function of $\tan\beta$ and M_{A^0} in hMSSM benchmark.

Current Exclusion

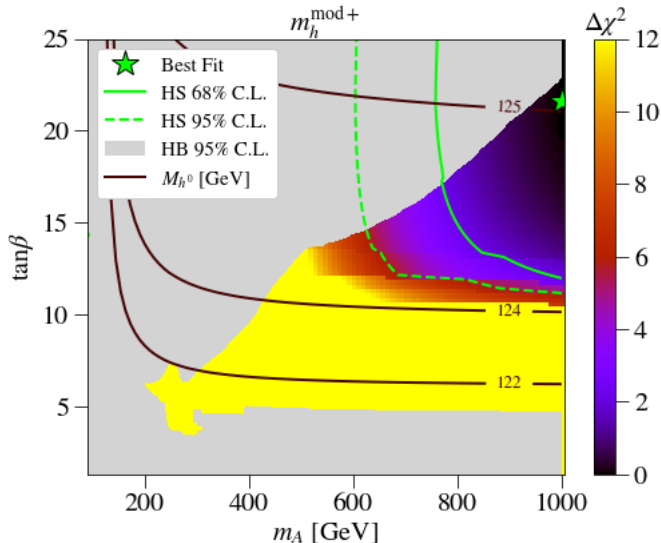


Figure: χ^2 fit sliced in the $\tan\beta$ and m_A plane in $m_h^{\text{mod+}}$ benchmark

Parameter Space

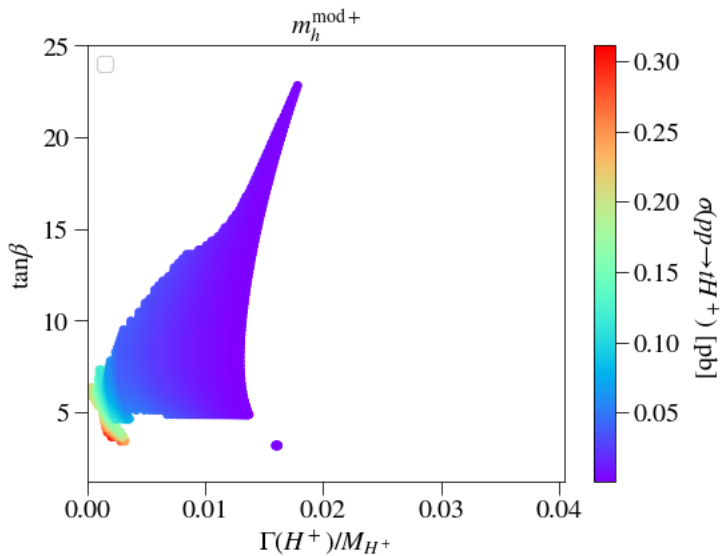


Figure: Cross section as a function of $\tan\beta$ and H^\pm width-mass ratio in $m_h^{\text{mod}+}$

Parameter Space

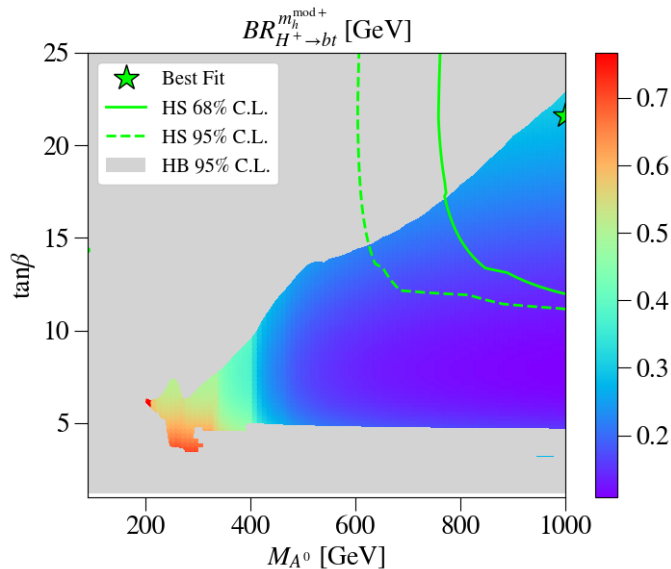


Figure: $Br(H^\pm \rightarrow tb)$ as a function of $\tan\beta$ and M_A^0 in m_h^{mod+} benchmark. Riley Patrick (UofA) Effects of Interference September 13, 2019 10 / 25

Parameter Space

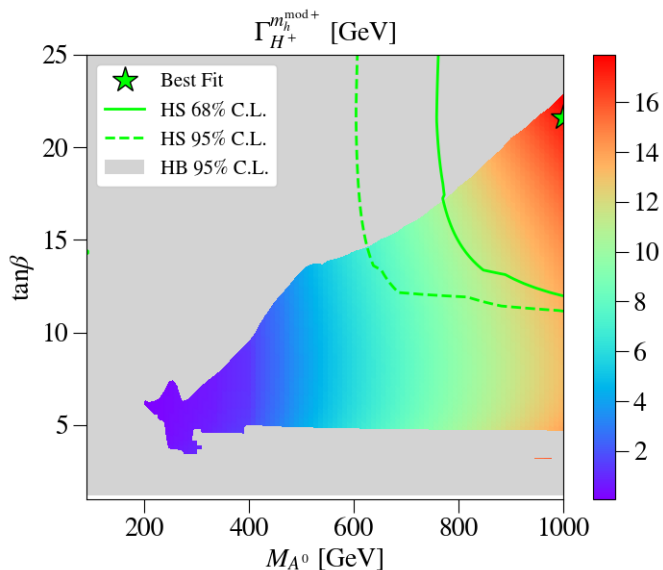


Figure: H^\pm width as a function of $\tan\beta$ and M_{A^0} in $m_h^{\text{mod+}}$ benchmark

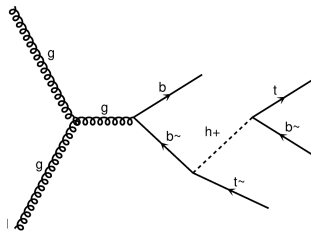
Benchmark Definition

Parameters	$h\text{MSSM}$	m_h^{mod+}
Masses in GeV		
M_{A^0}	125	113.55
M_{H^0}	648.3	298.69
M_{A^0}	628.79	292.22
M_{H^+}	633.91	303.08
$M_{S_1^+}$	119.63	133.2
$M_{S_2^+}$	280.37	274.19
$M_{\tilde{g}}$	1500	1500
$M_{\tilde{s}_1^0}$	71.72	80.637
$M_{\tilde{s}_2^0}$	138.35	143.88
$M_{\tilde{e}_1^0}$	285.39	276.42
$M_{\tilde{e}_2^0}$	1034.1	998.97
$M_{\tilde{\nu}_1}$	1038.6	1002.8
$M_{\tilde{\nu}_2}$	1532.7	1499.2
$M_{\tilde{d}_L}$	1532.7	1499.7
$M_{\tilde{d}_R}$	1532.7	1501
$M_{\tilde{u}_L}$	1532.7	1500.2
$M_{\tilde{u}_R}$	500.02	501.94
$M_{\tilde{e}_R}$	500.02	501.56
$M_{\tilde{\mu}_L}$	500.02	501.95
$M_{\tilde{\mu}_R}$	500.02	501.55
$M_{\tilde{e}_{cL}}$	499.96	496.48
$M_{\tilde{e}_{cR}}$	499.96	496.48
$M_{\tilde{\tau}_{cL}}$	999.98	998.25
$M_{\tilde{\tau}_L}$	1532.7	1501
$M_{\tilde{\tau}_R}$	1532.7	1500.2
$M_{\tilde{\chi}_1^0}$	998.34	1000.1
$M_{\tilde{\chi}_2^0}$	1001.8	1001.7
$M_{\tilde{\chi}_1^{\pm}}$	900.08	876.61
$M_{\tilde{\chi}_2^{\pm}}$	1173.8	1134.9
$M_{\tilde{a}_L}$	1532.7	1499.2
$M_{\tilde{a}_R}$	1532.7	1499.7
Total decay width in GeV		
$\Gamma(H^+)$	27.777	0.9253
$\Gamma(H^+)/M_{H^+}$	0.043819	0.0031
$BR(H^+ \rightarrow XY)$ in %		
$BR(H^+ \rightarrow b\bar{t})$	99.418	72.036
$BR(H^+ \rightarrow \tilde{\chi}_1^+ \tilde{\chi}_2^0)$	—	20.73
$BR(H^+ \rightarrow \tilde{\chi}_1^0 \tilde{\chi}_2^+)$	—	3.55
$BR(H^+ \rightarrow \tilde{\chi}_2^+ \tilde{\chi}_2^0)$	—	—
$BR(H^+ \rightarrow \tilde{\chi}_2^0 \tilde{\chi}_2^0)$	—	—
$BR(H^+ \rightarrow W^+ h^0)$	0.48	2.79
$BR(H^+ \rightarrow \tau^+ \nu_\tau)$	0.0048236	0.7682
Cross sections in pb		
$\sigma(pp \rightarrow tH^+)$	0.28622	0.2921
$\sigma(pp \rightarrow tH^+) \times BR(H^+ \rightarrow b\bar{t})$	0.28455	0.21042
$\sigma(pp \rightarrow tH^+) \times BR(H^+ \rightarrow \tilde{\chi}_1^+ \tilde{\chi}_2^0)$	—	0.0601
$\sigma(pp \rightarrow tH^+) \times BR(H^+ \rightarrow \tilde{\chi}_1^0 \tilde{\chi}_2^+)$	—	0.0104
$\sigma(pp \rightarrow tH^+) \times BR(H^+ \rightarrow \tilde{\chi}_2^+ \tilde{\chi}_2^0)$	—	—
$\sigma(pp \rightarrow tH^+) \times BR(H^+ \rightarrow \tilde{\chi}_2^0 \tilde{\chi}_2^0)$	—	—
$\sigma(pp \rightarrow tH^+) \times BR(H^+ \rightarrow W^+ h^0)$	0.0014	0.008
$\sigma(pp \rightarrow tH^+) \times BR(H^+ \rightarrow \tau^+ \nu_\tau)$	1.3806×10^{-5}	0.00201

Table 3: Benchmarks points for the two scenarios. We used $\tan\beta = 1, 01$ and 3.42 respectively for hMSSM and m_h^{mod+} .

Process and Key Parameters

- Model: hMSSM
- Key Parameters:
 - $\tan \beta = 1.01$
 - $M_{H^\pm} \approx M_A \approx M_H \approx 635$ GeV
 - $\Gamma_{H^\pm} \approx \Gamma_A \approx \Gamma_H \approx 27$ GeV
- Process: $pp \rightarrow tbH^\pm \rightarrow tb\bar{t}\bar{b}$



- Model: $m_h^{\text{mod}+}$
- Key Parameters:
 - $\tan \beta = 3.42$
 - $M_{H^\pm} \approx M_A \approx M_H \approx 303.08$ GeV
 - $\Gamma_{H^\pm} \approx \Gamma_A \approx \Gamma_H \approx 0.93$ GeV
- Process: $pp \rightarrow tbH^\pm \rightarrow tb\bar{t}\bar{b}$

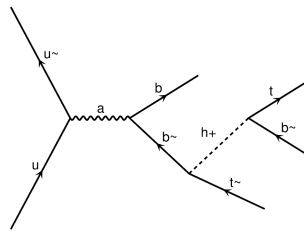


Figure: Examples of Production Diagrams for $tbtb$.

Monte Carlo

- MadGraph5 used to generate 20,000,000 parton level events.
- PYTHIA8 used on 500,000 of these events for fragmentation/hadronization.
- Delphes used on (the same) 500,000 events for detector effects.
 - Standard ATLAS card used

Event Reconstruction

- The following vetoes are applied:
 - $N_\ell = 1$, $N_j \geq 5$, $N_b \geq 2$ or 3
- Longitudinal momentum of missing energy solved using:

$$p_\nu^z = \frac{1}{2p_{\ell T}^2} \left(A_W p_\ell^z \pm E_\ell \sqrt{A_W^2 \pm 4p_{\ell T}^2 E_{\nu T}^2} \right)$$

where, $A_W = M_{W^\pm}^2 + 2p_{\ell T} \cdot E_{\nu T}$

- Reconstruction performed via simultaneous minimization of:

$$\begin{aligned} \chi_{\text{had}}^2 = & \frac{(M_{\ell\nu} - M_W)^2}{\Gamma_W^2} + \frac{(M_{jj} - M_W)^2}{\Gamma_W^2} + \frac{(M_{\ell\nu j} - M_T)^2}{\Gamma_T^2} \\ & + \frac{(M_{jjj} - M_T)^2}{\Gamma_T^2} + \frac{(M_{jjjj} - M_{H^\pm})^2}{\Gamma_{H^\pm}^2} \end{aligned}$$

- and the equivalent term for a leptonically decaying H^\pm .

Event Reconstruction

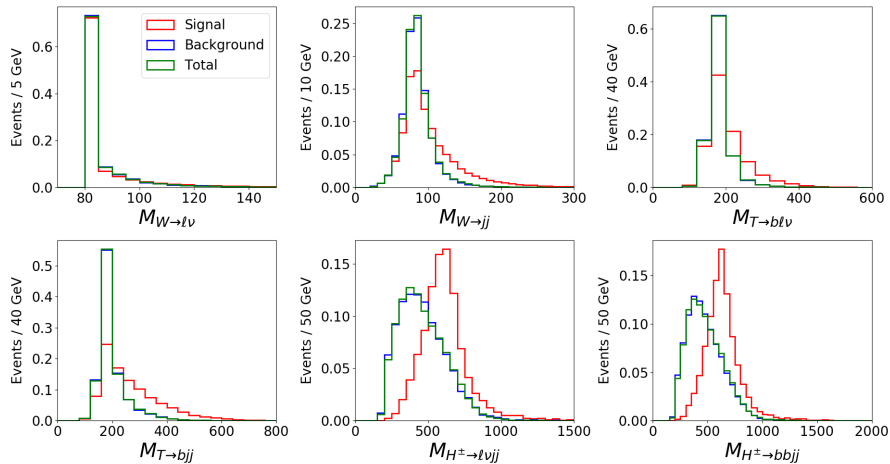


Figure: Invariant Mass distributions for reconstructed particles.

Parton Level Results

- The full 20,000,000 events used to achieve required statistics.

Model		S (pb)	B (pb)	S+B (pb)	I (pb)
hMSSM	σ	0.032402	13.078	13.139	0.028
	$\Delta\sigma$	1.4×10^{-5}	0.002	0.001	0.003
$m_h^{\text{mod}+}$	σ	0.088536	13.095	13.197	0.014
	$\Delta\sigma$	3.3×10^{-5}	0.001	0.001	0.002

Table: Parton level results for the hMSSM and $m_h^{\text{mod}+}$ benchmarks.

Detector Level Results

Cut	S	B	S+B	I
No cuts:	97206	39235500	39417000	84294
$N_\ell = 1$:	21663	9008470	9120699	90565
$N_J \geq 5$:	18193	5300323	5368595	50078
$N_{BJ} \geq 2$:	10858	2577379	2598762	10523
$\cancel{E} > 20 \text{ GeV}$:	10302	2382379	2393400	717
$\cancel{E} + m_T^W > 60 \text{ GeV}$:	10133	2320387	2331515	994
Cut	S	B	S+B	I
$N_{BJ} \geq 3$:	607	83571	82381	-1798
$\cancel{E} > 20 \text{ GeV}$:	575	78471	75680	-3366
$\cancel{E} + m_T^W > 60 \text{ GeV}$:	565	76901	74498	-2970

Table: Cut flow results presented in expected event yield with 3000fb^{-1} of luminosity for the hMSSM benchmark.

Detector Level Results

Cut	S	B	S+B	I
No cuts:	265620	39285000	39591000	40380
$N_\ell = 1$:	60173	9031228	9109097	17695
$N_J \geq 5$:	44820	5326260	5378833	7752
$N_{BJ} \geq 2$:	25457	2585345	2620528	9725
$\cancel{E}_T > 20 \text{ GeV}$:	23624	2387349	2420593	9620
$\cancel{E}_T + m_T^W > 60 \text{ GeV}$:	23008	2327636	2360811	10167

Cut	S	B	S+B	I
$N_{BJ} \geq 3$:	9692	835591	856749	11464
$\cancel{E}_T > 20 \text{ GeV}$:	8996	770771	791424	11655
$\cancel{E}_T + m_T^W > 60 \text{ GeV}$:	8754	752307	771628	10566

Table: Cut flow results presented in expected event yield with 3000fb^{-1} of luminosity for the $m_h^{\text{mod+}}$ benchmark.

Interference Shape

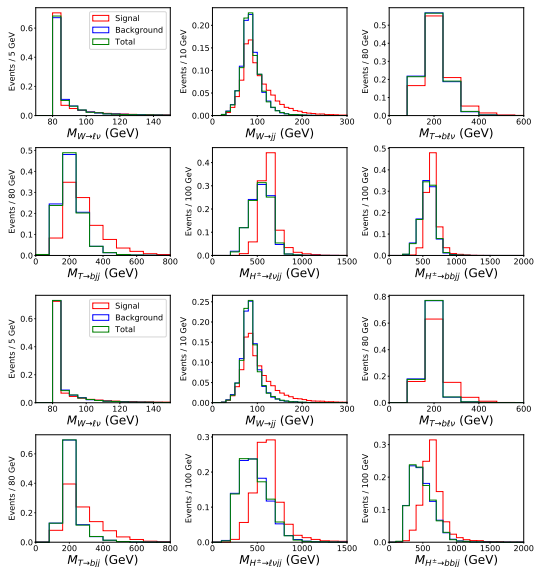


Figure: Invariant Mass distributions for reconstructed particles normalized to unit events.

Interference Shape

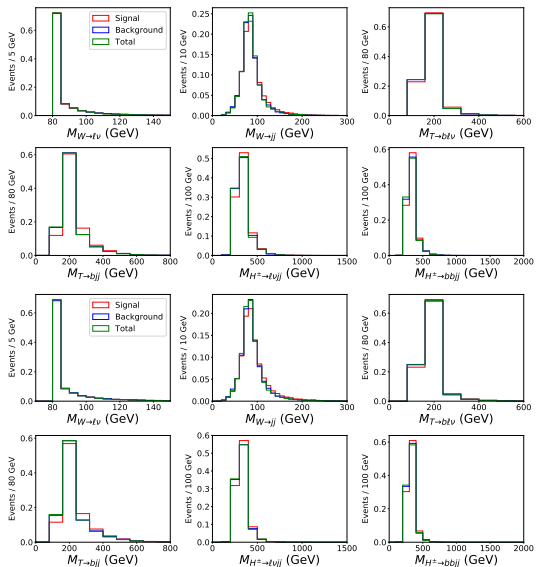


Figure: Invariant Mass distributions for reconstructed particles normalized to unit events.

Interference Shape

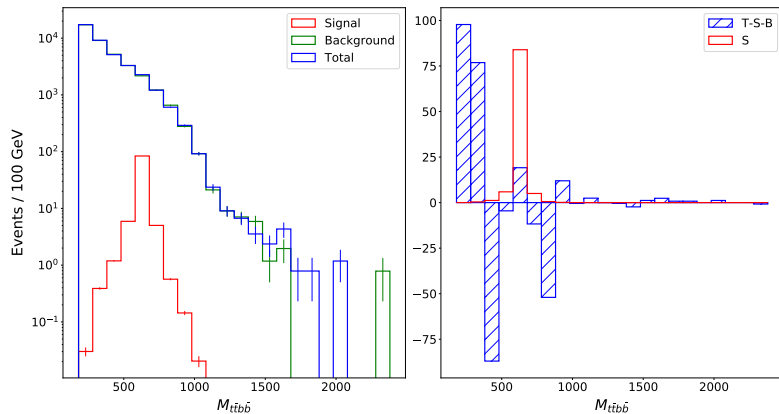


Figure: The charged Higgs invariant mass distribution of the signal, background as well as total (left) plus the interference and signal (right) at parton level and without cuts in the hMSSM scenario.

Interference Shape

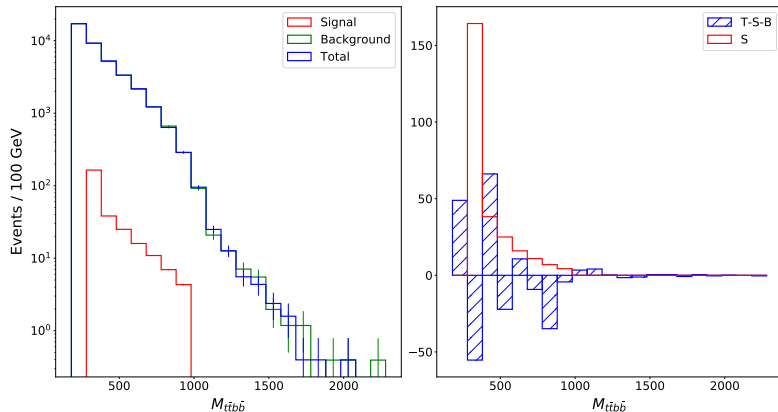


Figure: The charged Higgs invariant mass distribution of the signal, background as well as total (left) plus the interference and signal (right) at parton level and without cuts in the $m_h^{\text{mod+}}$ scenario.

Summary and Conclusion

- Interference effects non-negligible in some high width-mass ratio scenarios.
- To account for this we must model Signal, Background and Signal+Background separately.
- hMSSM presents significant interference in reasonable circumstance with high width-mass ratio.
- $m_h^{\text{mod}+}$ presents significant interference behaviour during cuts in low width-mass ratio.
- Parton and Detector level results of inclusive cross section presented.
- Results on detector level interference shapes presented.
- How does one design a machine learning framework that includes interference effects?
- How does interference effect the machine learning discriminant?

Thank You